

Quantitative ^{31}P NMR detection of oxygen-centered and carbon-centered radical species

Dimitris S. Argyropoulos,^{a,*} Hongyang Li,^a Armindo R. Gaspar,^a Kamilah Smith,^b
Lucian A. Lucia^a and Orlando J. Rojas^a

^aForest Biomaterials Laboratory, College of Natural Resources, North Carolina State University, Raleigh, NC 27695-8005, USA

^bDepartment of Chemistry, Pulp and Paper Research Centre, McGill University 3420 University Street Montreal, Que., Canada H3A 2A7

Received 18 November 2005; revised 2 February 2006; accepted 6 February 2006
Available online 28 February 2006

Abstract—Quantitative ^{31}P NMR spin trapping techniques can be used as effective tools for the detection and quantification of many free radical species. Free radicals react with a nitroxide phosphorus compound, 5-diisopropoxy-phosphoryl-5-methyl-1-pyrroline-*N*-oxide (DIPPMPPO), to form stable radical adducts, which are suitably detected and accurately quantified using ^{31}P NMR in the presence of phosphorus containing internal standards. Initially, the ^{31}P NMR signals for the radical adducts of oxygen-centered ($\cdot\text{OH}$, $\text{O}_2^{\cdot-}$) and carbon-centered ($\cdot\text{CH}_3$, $\cdot\text{CH}_2\text{OH}$, $\text{CH}_2\cdot\text{CH}_2\text{OH}$) radicals were assigned. Subsequently, the quantitative reliability of the developed technique was demonstrated under a variety of experimental conditions. The ^{31}P NMR chemical shifts for the hydroxyl and superoxide reaction adducts with DIPPMPPO were found to be 25.3, 16.9, and 17.1 ppm (in phosphate buffer), respectively. The ^{31}P NMR chemical shifts for $\cdot\text{CH}_3$, $\cdot\text{CH}_2\text{OH}$, $\cdot\text{CH}(\text{OH})\text{CH}_3$, and $\cdot\text{C}(\text{O})\text{CH}_3$ spin adducts were 23.1, 22.6, 27.3, and 30.2 ppm, respectively. Overall, this effort forms the foundations for a targeted understanding of the nature, identity, and mechanisms of radical activity in a variety of biomolecular processes.

© 2006 Elsevier Ltd. All rights reserved.

1. Introduction

For many years spin traps have been used to increase the stability of free radicals in order for them to be identified and detected by electron paramagnetic resonance (EPR) spectroscopy. Spin traps are highly reactive toward free radicals, thereby allowing the acquisition of abundant information on the production of such species in biological, biochemical, and chemical systems. Spin traps have been used quite extensively in the detection of oxygen-centered radicals, namely $\cdot\text{OH}$ and $\text{O}_2^{\cdot-}$, and carbon-centered radicals ($\cdot\text{CH}_3$, $\cdot\text{CH}_2\text{OH}$, $\cdot\text{CH}(\text{OH})\text{CH}_3$, and $\cdot\text{C}(\text{O})\text{CH}_3$).^{1–4} Most of these studies made use of EPR spectroscopy to detect and quantify the involved radical species.

Spin trapping entails the reaction of nitrones or nitroso spin traps (paramagnetic species) with unstable free rad-

ical systems, in order to form a more stable free radical (radical adduct), which can be detected by EPR spectroscopy or any other analytical method. Recent accounts⁵ have demonstrated that phosphorus-containing spin traps give rise to radical adducts that have longer half-lives compared to other spin traps. This fact can be used to expand the capability of EPR spectroscopy. Unfortunately, these radical adducts degrade with time, becoming diamagnetic and, therefore, EPR-undetectable. However, the presence of phosphorus within these systems allows for the use of ^{31}P nuclear magnetic resonance (NMR) spectroscopy to investigate the detailed chemistry of radical reactions in complex reaction systems. This technique was termed '*NMR spin trapping*' by Khramtsov et al.⁵ For NMR proposes, the radical adducts, after conversion into their final diamagnetic forms, are stable over a long period of time. This is particularly important for in vivo experiments in which the paramagnetic adducts are even more unstable, since biological systems have a high capability for bioreduction.

The use of phosphorus-containing spin traps allows for the detection of diamagnetic products by ^{31}P NMR without the complexity of multiple signal overlap spec-

Keywords: Free radicals; Hydrogen peroxide; Hydroxyl radicals; Superoxide radicals; Phosphorus; ^{31}P NMR; Quantitative analysis; Spin traps; Alkyl radicals; Hydroxyalkyl radicals; Internal standards.
*Corresponding author. Tel.: +1 919 515 7708; fax: +1 919 515 6302; e-mail: dsargyro@ncsu.edu

tra usually encountered when common nuclei, such as proton or carbon, are examined. Overall, however, a possible drawback of this technique could be the reduced sensitivity of NMR compared to that of EPR. This is partly overcome by the acquisition of more NMR signals with time.⁶

The novel spin trap 5-diethoxyphosphoryl-5-methyl-1-pyrroline-*N*-oxide (DEPMPO, an α -phosphorus-containing DMPO (5,5-dimethyl-1-pyrroline *N*-oxide) analogue) was first reported by Frejaville et al. in 1993.⁷ Since then, various accounts have shown that this phosphorus-containing spin trap can be used in conjunction with ³¹P NMR to detect various free radical species.⁵ Recently, another novel phosphorus compound containing nitroxide, the 5-diisopropoxy-phosphoryl-5-methyl-1-pyrroline-*N*-oxide (DIPPMPO), was investigated.⁸ The new compound shows outstanding performance compared to DMPO and DEPMPO toward radical analyses when used in conjugation with ³¹P NMR. More specifically, we will demonstrate here for the first time that the DIPPMPO/•OOH adduct is more stable than other traps toward superoxide (O₂^{•-}). Furthermore, we will show that ³¹P NMR signals for DIPPMPO/•OOH and DIPPMPO/•OH are readily distinguishable. On the other hand, DIPPMPO involves simple preparation and has higher partition coefficient ($K_p = 2.1$) compared to DMPO (0.1) or DEPMPO (0.06). This high partitioning enables the trapping experiments to be conducted in cellular or lipid-rich environments.

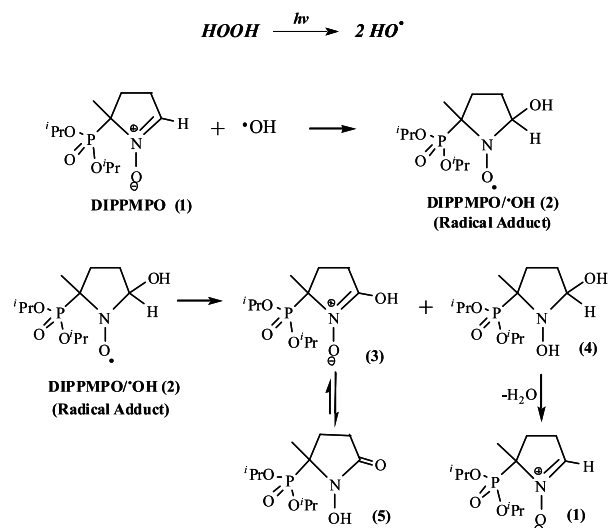
The stable diamagnetic products derived from the radical adducts coupled with the uniqueness of the quantitative ³¹P NMR technique can be exploited further to perform quantitative research work, because ³¹P NMR signal is specific to each trapped free radical. Consequently, our efforts in this paper are focused at detecting and quantifying oxygen- and carbon-centered radicals, which are important in biology, chemistry, and biochemistry, using phosphorus-containing spin traps and quantitative ³¹P NMR.

2. Results and discussion

2.1. Generation of oxygen-centered radicals

One common system to generate oxygen-centered radicals (•OH and O₂^{•-}) is the ultraviolet photolysis of hydrogen peroxide solutions. During this effort, the generated radicals were detected and quantified through their reaction with DIPPMPO. After the hydroxyl radicals are produced via ultraviolet photolysis of hydrogen peroxide, it takes place the spin trapping reaction between DIPPMPO (**1**) and hydroxyl radical producing the radical adduct DIPPMPO/•OH (**2**) (Scheme 1). A similar radical adduct was proposed by Khramstov et al.,⁵ when using DEPMPO as the spin trap.

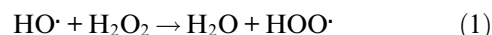
Once the concentration of the radical adducts increases, disproportionation and rearrangement reactions occur, affording a new nitron (**5**) and the original spin



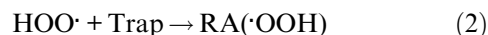
Scheme 1. Mechanism for the spin trapping of hydroxyl radicals using DIPPMPO.

trap (Scheme 1). As suggested by Khramstov et al.,⁵ in the course of spin trapping of hydroxyl radicals, the amount of new nitron (**5**) observed in the ³¹P NMR spectrum represents only half of the total spin trapped radical. The other half of the radical adducts that are initially formed (**2**) are transformed back into the original spin trap via the loss of water of the hydroxylamine product (**4**). Consequently, when quantification is required, the NMR integral of the corresponding radical adduct peak in the ³¹P NMR spectrum should be doubled.

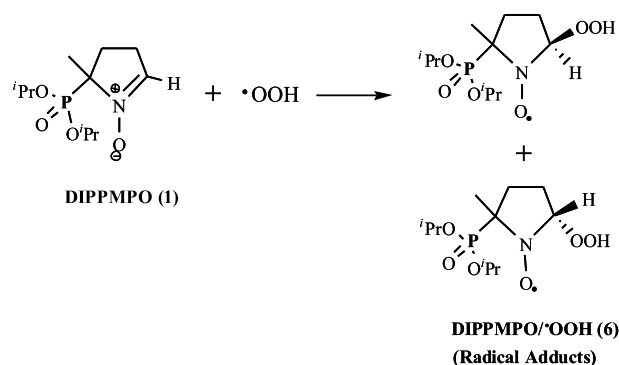
Hydroperoxyl radicals can be readily formed via the reaction of hydroxyl radicals and hydrogen peroxide in accordance with reaction (1):



The hydroperoxyl radical can then be trapped and form the hydroperoxyl radical adduct RA(•OOH):



Scheme 2 illustrates the spin trapping reaction between DIPPMPO and hydroperoxyl radicals.



Scheme 2. Spin trapping reaction between DIPPMPO and hydroperoxyl radicals.

The superoxide free radical can also react with the activated double bond of the spin trap resulting in the formation of hydroperoxide.⁹ However, the primary reaction of superoxide in aqueous media is disproportionation, which occurs at a faster rate than addition to a double bond.¹⁰ Disproportionation via hydrogen abstraction from solvent molecules, or other substrates, produces $\text{HOO}\cdot$, which then adds to the double bond of the nitron (1). It is therefore expected that the reaction product of superoxide with DIPPMPPO should indeed be a hydroperoxide. Despite the fact that the superoxide radical anion is a strong nucleophile in aprotic solvents, in protic solvents such as water it does not react as a nucleophile.¹¹ Consequently, nucleophilic addition of the superoxide radical anion to the double bond of the spin trap is not likely.

Literature accounts indicate that the trapping of superoxide with DEPMPO results in the formation of a ^{31}P NMR signal that cannot be distinguished from that of the hydroxyl reaction product.⁵ This finding was based on the fact that no new phosphorus resonances were observed in the spectrum, even though ESR measurements showed that the DEPMPO spin trap did indeed trap superoxide. The reported weak signals, as a result of trapping superoxide, were explained to be a consequence of superoxide radical adducts being reduced to their corresponding hydroxylamines and converted back into the original DEPMPO spin trap via the loss of hydrogen peroxide.⁵

Thus, the following account aims at identifying and accurately quantifying $\cdot\text{OH}$ or $\text{O}_2^{\cdot-}$ radicals, since distinct ^{31}P NMR signals for their trap adducts have been obtained through the use of DIPPMPPO as the spin trap.

2.2. Characterization of oxygen-centered radicals

2.2.1. Detection by ^{31}P NMR. As already discussed in light of Schemes 1 and 2, the species immediately formed after the spin trap reacts with a given radical are paramagnetic radical adducts. The lifetime of these paramagnetic species is finite. Furthermore, the disproportionation products, which are diamagnetic, can be observed by ^{31}P NMR as distinct sharp signals. A typical ^{31}P NMR spectrum obtained from the UV photolysis reaction of hydrogen peroxide (2.5 mol L^{-1}) in the presence of DIPPMPPO (68 mmol L^{-1}) is shown in Figure 1 (numbers refer to structures in Schemes 1 and 2). Measurements were taken 5–10 min after the irradiation of the sample was complete. The complete assignment of the ^{31}P NMR signals is presented in Table 1. This spectrum (Fig. 1) shows peaks that correspond to the radical reaction reduction products of $\cdot\text{OH}$ and $\text{O}_2^{\cdot-}$ radicals, supporting the mechanism of Scheme 2.

The ^{31}P NMR signal present at 25.3 ppm (Fig. 1) can unambiguously be assigned to the hydroxyl radical reaction product. The chemical shift difference between this signal and the DIPPMPPO resonance is 3.1 ppm upfield. This chemical shift difference closely agrees with the difference observed by Khrastov for DEPMPO and the DEPMPO/adduct reduction product that arises upon the trapping of hydroxyl radicals (3.4 ppm).⁵

Notably, when we use the Fenton system to generate radicals, only hydroxyl radicals were detected, since the ^{31}P NMR spectrum obtained from this reaction system contained no signal due to the DIPPMPPO/ OOH adduct. Furthermore, linear relationships were obtained for the hydroxyl radical formation when plotted versus the concentration of the Fenton system ($\text{H}_2\text{O}_2/\text{Fe}^{2+}$ as 1000:1) at pH 7 (Fig. 2). Even under different buffered

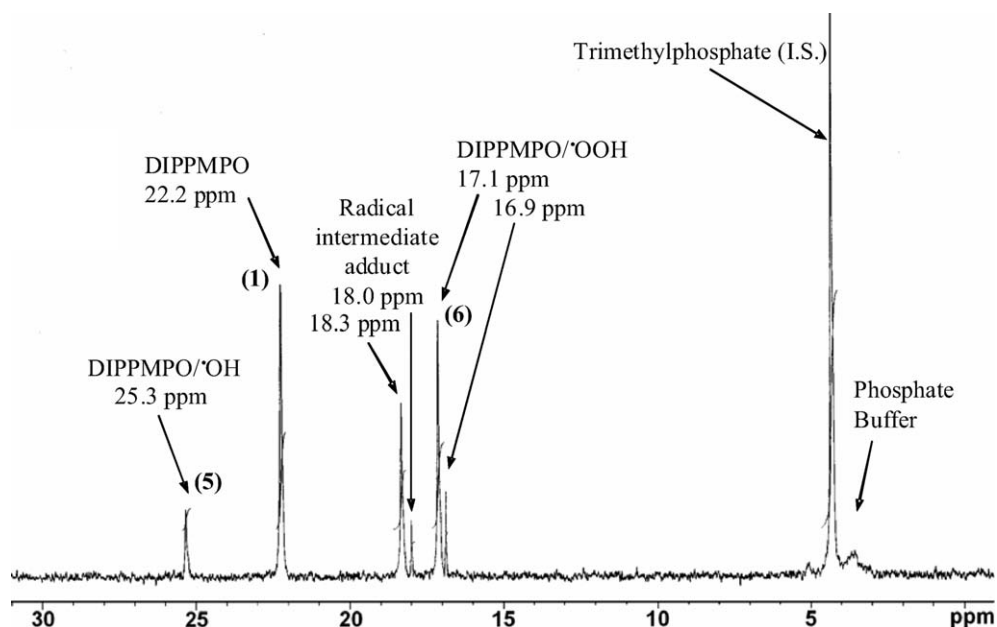


Figure 1. Quantitative ^{31}P NMR spectrum of the products formed from the UV photolysis of H_2O_2 in a sodium hydrogen phosphate buffer solution (pH 7.4). I.S. (internal standard) = trimethylphosphate.

Table 1. ^{31}P NMR signals for DIPPMPPO reaction adducts

Species	Generating System	Chemical shift (ppm)
DIPPMPPO (1)		22.2
DIPPMPPO/OH (5)	8% H_2O_2 + UV light Fenton reaction: $\text{Fe}^{2+} + \text{H}_2\text{O}_2 + \text{DTPA}$	25.3
DIPPMPPO/OOH (6)	8% H_2O_2 + UV light $\text{H}_2\text{O}_2 + \text{O}_2 + \text{OH}^-$	16.9, 17.1
Intermediate radical species	8% H_2O_2 + UV light $\text{H}_2\text{O}_2 + \text{O}_2 + \text{OH}^-$	18.0, 18.3

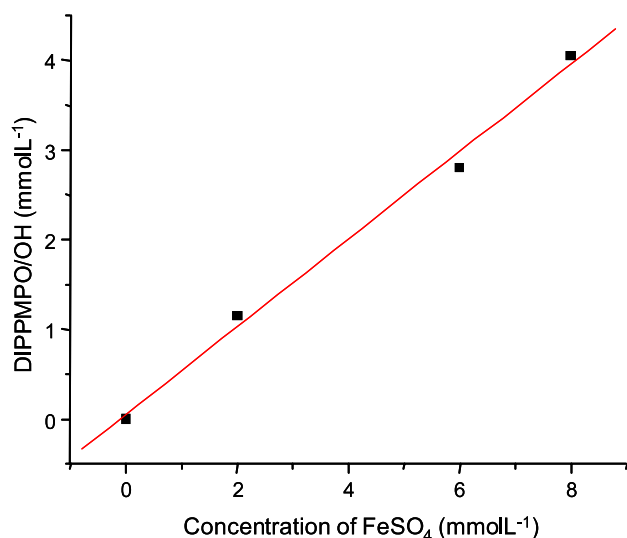


Figure 2. Concentration of hydroxyl radical trapped as a function of the Fenton system concentration ($\text{H}_2\text{O}_2/\text{Fe}^{2+}$ as 1000:1) at pH 7. DIPPMPPO (30 mmol L^{-1}) was added to trap the radicals. ^{31}P NMR was used to provide the quantitative analysis results after the mixture was stirred continuously under air in the dark for 120 min.

conditions for pH's (pH 2, 7, 9, and 13), those linear relationships were still apparent.

It is important to note that unlike DMPO, the superoxide/hydroperoxyl radical adducts of DEPMPPO (DEPMPPO/OOH), and DIPPMPPO (DIPPMPPO/OOH), do not decompose to give DIPPMPPO/OH. False DIPPMPPO/OH signals are therefore not a problem by this method.¹ The DIPPMPPO/OH radical adduct is only formed from the reaction between DIPPMPPO and $\cdot\text{OH}$ radicals in the system. When DMPO was used as the spin trap, the formation of DMPO/OH included some false adduct arising from the UV irradiation or water via the reaction of DMPO and H_2O catalyzed by metal ions.⁸ However, for the case of DIPPMPPO, the DIPPMPPO/OH adduct is only created from hydroxyl radicals, formed from the UV photolysis of H_2O_2 , and not from the water solvent. Lloyd et al.¹¹ have carried out spin trapping experiments with 30% hydrogen peroxide and labeled water (^{17}O) in which they proved that exchange between water solvent and H_2O_2 does not occur.

Besides the DIPPMPPO/OH adduct, the DIPPMPPO/OOH adduct was also found to be present in the products of the UV photolysis of hydrogen peroxide. The ^{31}P NMR signal induced by the hydroperoxyl rad-

ical adduct is located at 17.1 ppm (Fig. 1). The photolysis of H_2O_2 , at shorter ultraviolet irradiation times, has shown two singlets at 17.1 and 18.0 ppm. However, as the time of irradiation increased, two new signals appeared at 16.9 and 18.3 ppm. The ^{31}P NMR signals at 18.0 and 18.3 ppm most likely represent various other radical species, intermediates in the overall reaction mechanism, whose precise identity is currently under investigation. The signals at 16.9 and 17.1 ppm have been assigned to superoxide reaction products.¹² The assignment of these signals to superoxide products was further verified using DIPPMPPO in an alkaline hydrogen peroxide system that is known to generate superoxide.¹³

Potassium superoxide (KO_2), when dissolved in water, is known to generate superoxide¹² which can then be trapped and consequently its phosphorus signal detected. The spectrum that resulted from this reaction contained a ^{31}P NMR signal at 17.1 ppm along with several unidentified peaks whose identities are currently under examination. The presence of this signal in the superoxide generating system, along with the observation that this signal was drastically reduced when the enzyme superoxide dismutase (SOD) was introduced into the system, further confirms that the peak at 17.1 ppm is related to the presence of $\text{O}_2^{\cdot-}$. Superoxide dismutase accelerates the rate of superoxide radical dismutation to hydrogen peroxide, therefore a dose-dependent diminution in the spectrum should be observed if the signal is due to the presence of superoxide radical anion.¹²

It has been shown that superoxide radicals can be formed in good yield by the photolysis of hydrogen peroxide solutions.¹⁴ Therefore, signals due to the spin trapping of hydroxyl radicals and superoxide radicals were anticipated in the ^{31}P NMR spectrum of such reactions. It is likely that the signals at 16.9 and 17.1 ppm correspond to the two diastereomeric forms of the reaction product of DIPPMPPO with superoxide, since the carbon in position 2 is chiral (Scheme 2).¹⁴

The X-ray structure of DIPPMPPO shows that the position of the diisopropoxyphosphoryl group induces larger steric hindrance of the nitron face, although the isopropoxyl substituents are oriented toward the exterior of the ring.⁸ This steric hindrance that favors *trans* radical addition to the phosphoryl group should be particularly important in water because of solvation. For this reason, the signals for carbon-centered radicals ($\cdot\text{CH}_3$, $\cdot\text{CH}_2\text{OH}$, $\cdot\text{CH}(\text{OH})\text{CH}_3$ or $\cdot\text{C}(\text{O})\text{CH}_3$) are antic-

ipated to show only one ^{31}P NMR signal (see Section 2.4).

The stereoselectivity and stereospecificity of radical addition to nitrones are known.¹⁵ More specifically, it has been reported that superoxide radical additions to DEPMPO are stereoselective, while hydroxyl radicals are trapped stereospecifically.^{16,17} Frejaville et al.¹⁸ have also reported on the stereospecificity of DEPMPO with a variety of other radicals such as $\text{CO}_2^{\cdot-}$, $\text{SO}_3^{\cdot-}$, $\cdot\text{CH}_3$, and α -hydroxyalkyls in aqueous media. These researchers have also shown that in phosphate buffers at pH 5.6 and 7.0 the superoxide adduct of DEPMPO is stereoselective.¹⁹ From these latter findings, it follows that spin trapping experiments should result in the formation of both superoxide radical adducts and only one isomer of the hydroxyl spin adduct. This is indeed the case with the DIPPMPPO spin trap, since we observed a single resonance corresponding to the trapping of hydroxyl radicals and two signals due to the trapped superoxide. For the formation of superoxide radical through the UV photolysis of H_2O_2 at shorter reaction times, only one peak appeared, which is most likely due to the fact that at shorter irradiation times only the major stereoisomer of the superoxide adduct is prevalent. At longer times, there is an accumulation of the minor stereoisomer, which is then also detected.

The structure of the superoxide radical adduct, which induces the aforementioned ^{31}P NMR signals at 16.9 and 17.1 ppm, was also elucidated by carrying out GC/MS analyses of freeze-dried samples. The major peak at $m/z = 254$ corresponds to the loss of the isopropyl group. MS/MS analysis was also performed on these samples and the m/z for these signals was determined to be 297, in agreement with the results obtained from GC/MS analysis.

2.2.2. Examining the quantitative reliability for oxygen-centered radicals. Spin trapping experiments used to determine the concentrations of the various free radicals were performed at least three times in order to examine the quantitative reliability of the developed techniques. UV irradiations of 2.5 mol L^{-1} hydrogen peroxide solutions were used to generate hydroxyl radicals. The experiments were performed at pH 7.4, using a phosphate buffer solution, and 4 mmol L^{-1} of diethylenetriaminepentaacetic acid (DTPA) was used to remove metal impurities from the samples. The metal-chelating agent DTPA was used since the major source of error that can be associated with this spin trapping is the presence of trace metal impurities, especially in buffered solutions. The concentration of radical species was monitored as a function of time using an internal standard followed by quantitative ^{31}P NMR spectroscopy.

The concentration of hydroxyl radicals produced and trapped by DIPPMPPO was measured as a function of total irradiation time. Figure 3 shows that under the UV photolysis conditions, the concentration of hydroxyl radicals produced and trapped is linear with time. The apparent rate of hydroxyl radical production for these experiments was found to be $0.200 \text{ mmol min}^{-1}$. These

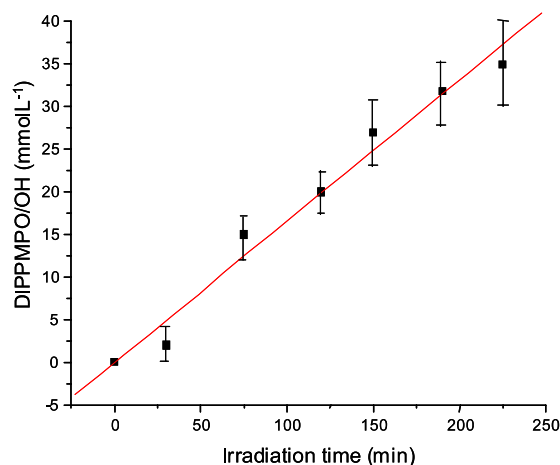


Figure 3. Concentration of hydroxyl radicals trapped as a function of total ultraviolet irradiation time for 2.5 mol L^{-1} hydrogen peroxide solutions containing DIPPMPPO (68 mmol L^{-1}) spin trap. Discrete data points represent the integral intensity for the ^{31}P NMR signal at 25.3 ppm. Data points shown are averages of triplicate experiments. Apparent Rate Constant = $0.200 \text{ mmol L}^{-1} \text{ min}^{-1}$ ($R^2 = 0.97$).

data are in accord with previous EPR experiments that have shown that when high concentrations of DEPMPO are used, the rate of spin trapping of hydroxyl radical generation is linear with time.¹⁹

The apparent increase in the error distribution at extended irradiation times warrants attention. A source of error is associated with the residual amounts of metals present. Besides the use of DTPA in the spin trapping experiments, there are always residual amounts of metals that will lead to related errors. Another source of error could be the amount of dissolved oxygen in the samples. The concentration of free radicals in the peroxide solutions, namely superoxide radicals which can decompose to provide hydroxyl radicals, is influenced by the concentration of molecular oxygen present in the sample. These sources of possible errors can add during irradiation, which explains why the associated standard deviation increases with the time of UV photolysis of H_2O_2 (see Fig. 3).

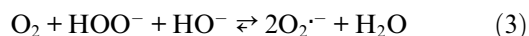
2.3. Quantification of superoxide/hydroperoxyl radicals

2.3.1. Generation of the superoxide/hydroperoxyl radicals. Our efforts to develop a new superoxide/hydroperoxyl quantitative analytical method, which can be directly used for the study of organic radical processes, demanded an effective generation system of superoxide radical.

When the photolysis of H_2O_2 is used to generate the superoxide radicals, hydroxyl spin adducts are also formed. The different radical species formed from the UV photolysis of hydrogen peroxide make the quantitative analysis of superoxide radicals dependent on several conditions. Besides the photolysis of H_2O_2 , potassium superoxide in water or enzyme systems can be used to generate the superoxide radicals. Potassium superoxide

(KO₂), when dissolved in water, is known to generate superoxide¹² which can then be trapped along with several other yet unidentified radical species. This mixture of products may complicate the analysis of the single superoxide radical. Enzyme systems can be also used to form superoxide radicals effectively and reliably. For this reason they are frequently used in spin trapping experiments followed by EPR measurements.²⁰ However, the concentration of the superoxide radicals generated from enzyme systems is very low. Taking into account the detection limits of NMR, the detection of such radical adducts could be problematic.

In our efforts to overcome these deficiencies, we used a novel superoxide generation reaction, recently proposed by Petlicki and van de Ven.¹³ These authors have proposed that superoxide radicals should form when alkaline hydrogen peroxide is in contact with oxygen, as described by the following equation.



In fact, we determined this method of superoxide radical generation to be an effective system that allowed further expanding the scope of our work. Consequently, we examined and explored the various reaction conditions on the superoxide/hydroperoxide formation.

2.3.2. Influence of DIPPMPPO concentration on the DIPPMPPO/OOH adduct generation. The effect of the DIPPMPPO concentration on the DIPPMPPO/OOH adduct generation was evaluated within the range 50–500 mmol L⁻¹ of DIPPMPPO, using, in all cases, 300 mmol L H₂O₂ (Fig. 4). With increasing concentration, up to 200 mmol L⁻¹ of spin trap, the concentration of DIPPMPPO/OOH radical adduct was also increased. These series of measurements demonstrated that the actual amount of superoxide trapped was dependent on the DIPPMPPO concentration up to about 200 mmol L⁻¹. Beyond this point, the radical adduct

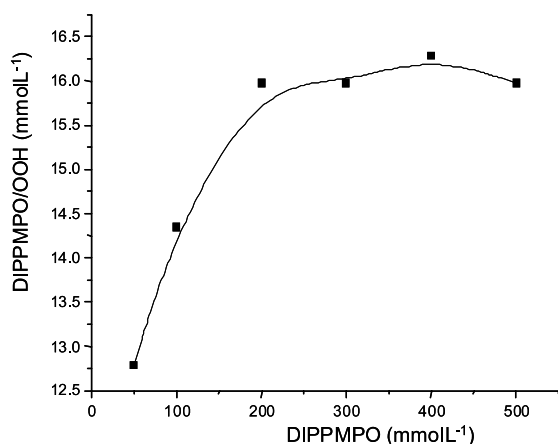


Figure 4. Concentration of DIPPMPPO/OOH as a function of concentration of DIPPMPPO. DIPPMPPO (50–500 mmol L⁻¹) was added to trap the radicals at a buffered environment of pH 8.8. ³¹P NMR was used to quantify DIPPMPPO/OOH after the mixture was stirred continuously under air in the dark for 20 min.

produced was found to be constant, indicative of reaction completion.

When DEPMPO is used, the intensity of the superoxide adduct signal was found to decrease with an increasing concentration of the spin trap. The maximum intensity of DEPMPO/OOH signal obtained was at 10 mmol L⁻¹ DEPMPO. On the other hand, the concentration of carbon-centered radical increases with the concentration of the DEPMPO used up to 50 mmol L⁻¹. Similar tendencies were observed when DMPO is used as the spin trap.²¹

2.3.3. Superoxide radical generation as a function of H₂O₂ concentration. The amount of superoxide radicals produced and trapped by DIPPMPPO was also measured as a function of the H₂O₂ concentration. Figure 5 shows that under the conditions used (see Section 4), the concentration of superoxide radicals produced and trapped is linear with the initial concentration of H₂O₂, i.e., the generation of superoxide radical is directly proportional to the amount of the H₂O₂ present in the system.

2.3.4. Kinetic analysis of the DIPPMPPO/OOH adduct generation. The superoxide radical generation, as described by Eq. 3, measured by the DIPPMPPO/OOH adduct, was found to linearly increase for the ca. 200 min from the onset of the reaction (Fig. 6). For the time interval 0–200 min, the superoxide radical production was found to follow a pseudo-zero-order reaction with a rate constant of 0.4 mmol L⁻¹ min⁻¹.

Beyond ca. 200 min time the radical adduct production levels off (Fig. 6). One possible explanation for this could be due to the concentration of the spin trap used (100 mmol L⁻¹). Beyond 200 min, the concentration of superoxide radicals trapped was found to be about 70 mmol L⁻¹. This amount of radical adduct is near

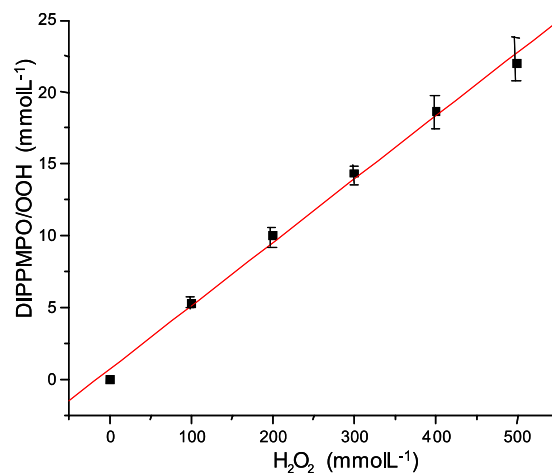


Figure 5. Concentration of superoxide radicals trapped as a function of concentration of H₂O₂. DIPPMPPO (100 mmol L⁻¹) was added to trap the radicals at pH 8.8. ³¹P NMR was used to provide the quantitative analysis results after the mixture was stirred continuously under air in the dark for 20 min. All measurements were carried out in triplicate (linear relationship as $Y = 0.683 + 0.0441X$; with a $R^2 = 0.995$).

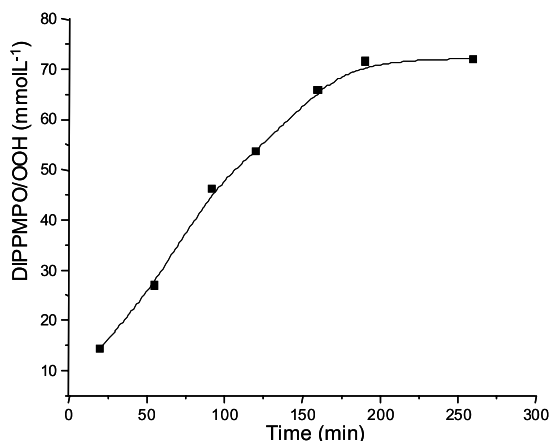


Figure 6. Concentration of superoxide radicals trapped as a function of time. DIPPMPPO (100 mmol L⁻¹) was added to trap the radicals at pH 8.8. ³¹P NMR was used to arrive at the quantitative data after the mixture was stirred continuously under air in the dark for up to 270 min.

the theoretical limit imposed by the initial concentration of DIPPMPPO used.

2.3.5. Activation energy in the formation of DIPPMPPO/OOH spin adducts. The activation energy in the generation of DIPPMPPO/OOH spin adducts was determined with reactions carried out at different temperatures (Fig. 7), in order to illustrate the dependence of the spin adduct formation with the temperature. With the increase of the reaction temperature, the amount of DIPPMPPO/OOH generated was also seen to increase. In the temperature range 28–50 °C, DIPPMPPO/OOH was found to follow an almost linear increase, with a rate constant of about 1.2 mmol L⁻¹ °C⁻¹. Above 50 °C, the increase of the DIPPMPPO/OOH concentration with temperature became less obvious.

The activation energy was determined based on the Arrhenius equation assuming that the radical adduct

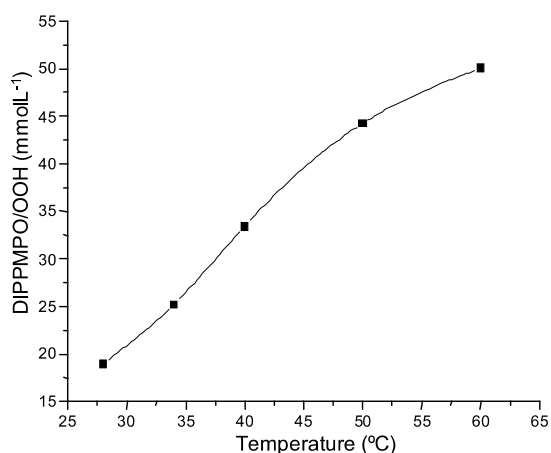
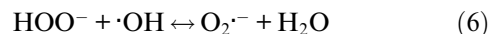
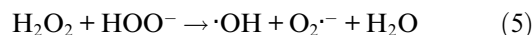
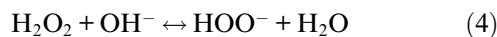


Figure 7. Concentration of superoxide radicals trapped as a function of temperature. DIPPMPPO (100 mmol L⁻¹) was added to trap the radicals at pH 8.8 within the temperature range 28–60 °C. ³¹P NMR was used in the quantification of concentrations after the mixture was stirred continuously under air in the dark for 20 min.

formation follows a pseudo-zero-order reaction (valid up to 60 °C). The activation energy for the formation process of superoxide radical adduct under the examined conditions was 33 kJ/mol ($R^2 = 0.98$).

2.3.6. Radical species in H₂O₂ solution as a function of pH. The distribution of the various free radicals present in solutions of hydrogen peroxide was examined as a function of pH. Figure 8 illustrates the increase in superoxide radical concentration with increasing pH. As anticipated, superoxide radicals were not detectable under acidic conditions. However, beyond pH 6 the formation of superoxide radicals was found to markedly increase with pH. In contrast, the concentration of hydroxyl radicals trapped did not vary as profoundly with pH compared to superoxide (Fig. 8). Furthermore, there were no detectable amounts of hydroxyl radicals trapped at pH 4 or 6. Evidently, the maximum quantity of hydroxyl radicals trapped was found to be around neutrality, followed by a slight decrease as the alkalinity was increased.

The increase in superoxide radical concentration as pH increases can be explained easily. The following equations elucidate the increase of superoxide radicals with increasing OH⁻ concentrations:



In the absence of transition metal ions, peroxide decomposition is a pH dependent, bimolecular reaction that involves the hydroperoxyl anion. An increase in superoxide radical concentration as a function of pH is expected since in alkaline conditions peroxide decomposes via various free radical intermediates (one of

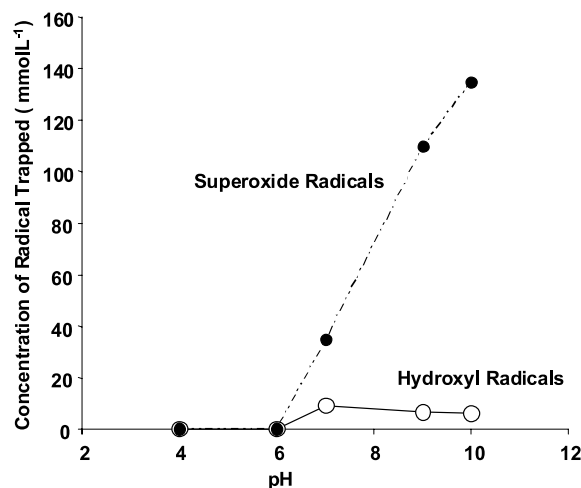


Figure 8. Concentration of radical species (³¹P NMR) trapped as a function of pH. DIPPMPPO (100 mmol L⁻¹) was added to trap the radicals. The data correspond to the mixture continuously stirred under air in the dark for 90 min.

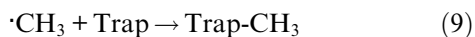
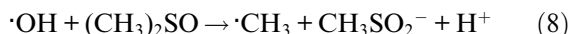
which is the superoxide radical) to yield water and molecular oxygen.²²

As one moves to more alkaline pH's more of the hydrogen peroxide in the system will be in the form of its conjugate base ($pK_a(H_2O_2) = 11.8$), therefore the formation of superoxide radical anion should be more significant. The hydroxyl radicals formed during the base-catalyzed decomposition of peroxide can subsequently react with hydroperoxyl anions to give hydroperoxyl and superoxide radicals:



2.4. Characterization of carbon-centered radicals

2.4.1. Generation of carbon-centered radicals. In order to generate carbon-centered radicals, solvents such as ethanol and dimethylsulfoxide can be added to a system with $\cdot OH$ present. Methyl radicals were generated either by the photolysis of *tert*-butylhydroperoxide or through scavenging reactions of hydroxyl radicals with dimethylsulfoxide (DMSO). The methyl radicals were generated using the $\cdot OH$ -dependent oxidation of DMSO in dilute hydrogen peroxide as described by the following equations:



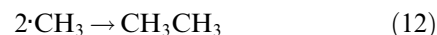
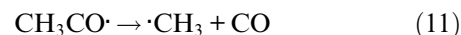
These radicals were trapped using both DEPMPO and DIPPMPPO spin traps. The MS spectrum for the spin trapping of $\cdot CH_3$ with DIPPMPPO demonstrates the nature of the radical adduct. The initial two fragmentations are due to the losses of the *i*-propyl groups.

2.4.2. Hydroxyalkyl and acyl radicals. In order to produce hydroxyalkyl radicals, hydrogen peroxide was combined with the appropriate alcohol and the sample was irradiated with ultraviolet light.²³ These solvents are hydroxyl radical scavengers that form carbon-centered radicals. Hydroxymethyl ($\cdot CH_2OH$) and α -hydroxyethyl ($\cdot CH(OH)CH_3$)²⁴ radicals can be readily formed if methanol and ethanol are introduced in a reaction system in the presence of hydroxyl radicals. We found that the ³¹P NMR chemical shifts for the diamagnetic disproportionation products were 22.6 and 27.3 ppm, respectively. In this work, the ³¹P NMR signals for the intermediate hydroxylamines that are formed, when dismutation occurs after the hydroxyalkyl radical has been trapped, were negligible. In previous work by Frejaville et al.,¹⁹ nitron and two stereoisomeric hydroxylamine signals were observed in the ³¹P NMR spectra for reactions in which $\cdot CH_2OH$ was trapped. In their work, the nitron degradation product for this radical was shifted 0.4 ppm downfield from the parent spin trap (DEPMPO). In the present study, the nitron formed by trapping $\cdot CH_2OH$ also appears at a chemical shift difference of 0.4 ppm downfield from the DIPPMPPO spin trap.

It has been reported that spin trapping of the α -hydroxyethyl radical in organic solvents does result in the production of two EPR spectra that correspond to diastereomeric isomers.²⁵ However, it has been observed by Pou et al.²⁶ that in EPR experiments in which the α -hydroxyethyl radical was generated in aqueous solution, diastereomeric isomers are not observed. In this work, only one resonance at 27.3 ppm was observed for the spin trapping of $\cdot CH(OH)CH_3$.

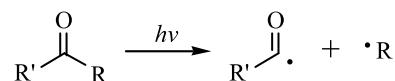
Aldehydes and ketones absorb in the 230–330 nm region. This is due to the π – π^* singlet–singlet transition.²⁷ Thus, aldehydes and ketones excited by ultraviolet light can cleave and generate free radical species (Scheme 3).

The cleavage reaction of ketones expressed in Scheme 3 is known as Norrish Type I cleavage. It is possible for R' to be formed via secondary processes that result in the acyl radical ($R'-CO\cdot$) losing carbon monoxide, schematically represented by the following reactions:



In order to produce methyl acyl radical ($\cdot C(O)CH_3$), acetone was irradiated with ultraviolet light in the presence of DIPPMPPO and the ³¹P NMR spectrum subsequently obtained. Figure 9 clearly indicates the presence of two ³¹P NMR signals that correspond to the DIPPMPPO spin trap (22.2 ppm) and most likely to the nitron formed when ethyl acyl radical is trapped.

Mass spectroscopy was also used to conclusively prove that the signal observed at 30.2 ppm corresponds to the structure shown in Figure 9. Unfortunately, MS/MS as well as GC/MS did not reveal any species that possessed a molecular ion at 305. The only molecular ion observed was 263, which corresponds to the original DIPPMPPO spin trap. It is likely that during MS analysis, under the conditions used, the structure readily fragmented producing species with a *m/z* of 263 (DIPPMPPO) and 43 (acyl group). The presence of a distinct ³¹P NMR signal at 30.2 ppm is therefore only assumed to be that of the nitron formed when ethyl acyl radical is trapped by DIPPMPPO, since under ultraviolet irradiation of the symmetric ketone, acetone should afford $\cdot C(O)CH_3$. Further work in this area with acetone and other ketones is consequently ongoing for clarifying this important issue.



Scheme 3. Cleavage of aldehyde or ketone using ultraviolet light.

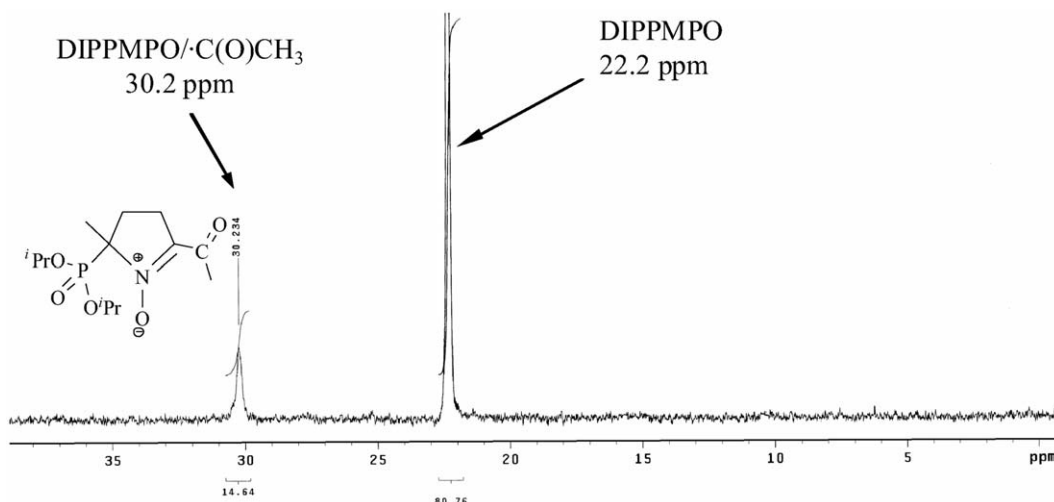


Figure 9. ^{31}P NMR spectrum of the nitron formed from the UV photolysis of acetone with DIPPMPPO spin trap.

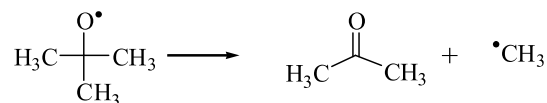
Table 2. ^{31}P NMR signals for DIPPMPPO carbon-centered reaction adducts

Species	Generating system	Chemical shift (ppm)
DIPPMPPO		22.2
DIPPMPPO/ CH_3	DMSO + 3% H_2O_2 + UV light	23.1
	$t\text{-BuOOH}$ + UV light	
DIPPMPPO/ CH_2OH	Methanol + 3% H_2O_2 + UV light	22.6
DIPPMPPO/ $\text{CH}(\text{OH})\text{CH}_3$	Ethanol + 3% H_2O_2 + UV light	27.3
DIPPMPPO/ $\text{C}(\text{O})\text{CH}_3$	Acetone + UV light	30.2

Table 2 is a summary of the ^{31}P NMR signals for the reaction products of DIPPMPPO with various carbon-centered free radical species.

2.4.3. Examining the quantitative reliability for methyl radical detection. UV photolysis of the organic peroxide, *tert*-butylhydroperoxide (30% *tert*-butylhydroperoxide by weight in water), was also carried out as a function of time. This reaction did not generate the *tert*-butoxy radical, $\text{O}(\text{CH}_3)_3$, but rather the methyl radical, CH_3 . This is expected since tertiary alkoxy radicals predominantly fragment into alkyl radicals and carbonyl species via intramolecular rearrangements,²⁸ as described in Scheme 4.

Figure 10 illustrates that the relationship of the concentration of generated methyl radicals is linear with respect to the total irradiation time. The apparent rate constant for this reaction was determined to be $0.20 \text{ mmol L}^{-1} \text{ min}^{-1}$. It is apparent from the graph that the regression line does not go through the origin. This is most likely due to the fact that the methyl radicals formed are the result of secondary reactions. The *tert*-butoxy radical is formed initially; however, subsequently the rearrangement of this radical into acetone and the methyl radical occurs. In Figure 9 are shown the detectable methyl radicals from the rearrangement reactions of $\text{O}(\text{CH}_3)_3$, which do not occur until approximately 100 min.



Scheme 4. Decomposition of the *tert*-butoxy radical into ketone and the methyl radical.

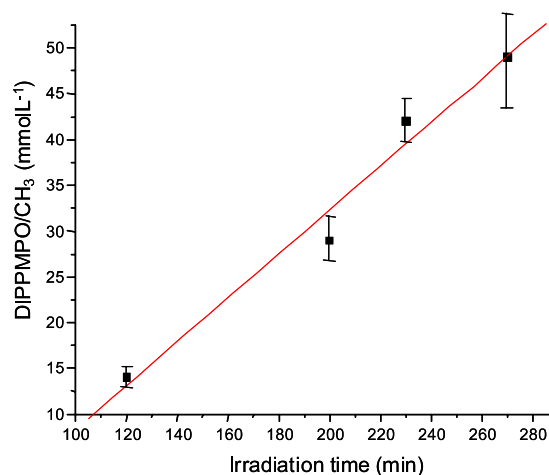


Figure 10. Concentration of methyl radicals trapped as a function of total ultraviolet irradiation of *tert*-butyl hydroperoxide solutions containing DIPPMPPO spin trap. Apparent rate constant = $0.20 \text{ mmol L}^{-1} \text{ min}^{-1}$ ($R^2 = 0.98$).

3. Conclusions

This work demonstrates that DIPPMPPO spin trapping, when used in conjunction with quantitative ^{31}P NMR, is an effective tool for the identification and quantification of oxygen- and carbon-centered free radical species. Using this technique, the radical adduct reduction products of a variety of free radical species can be detected. Hydroxyl and superoxide/hydroperoxide radicals, trapped with DIPPMPPO, were detected and quantified with the use of a phosphorus-containing internal standard. The chemical shifts for hydroxyalkyl and acyl radicals were also determined using the developed NMR spin trapping technique. The concentration of hydroxyl, methyl radicals, and *tert*-butyl hydroperoxide was determined as a function of ultraviolet irradiation time. The concentration of superoxide radicals was determined reproducibly as a function of hydrogen peroxide concentration. Apparent rate constants for hydroxyl and *tert*-butyl hydroperoxide radicals generated from the photolysis of hydrogen peroxide were determined to be $0.200 \text{ mmol L}^{-1} \text{ min}^{-1}$ in both cases. The rate constant for the superoxide radical formation was determined to be $0.400 \text{ mmol L}^{-1} \text{ min}^{-1}$.

4. Experimental

4.1. Reagents

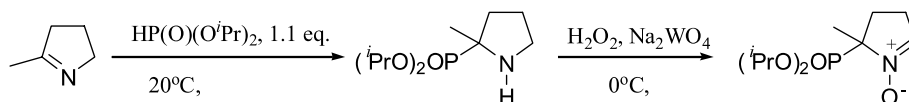
Diethylenetriaminepentaacetic acid (DTPA), potassium superoxide (KO_2), 30% (w/w) hydrogen peroxide, 3% (w/w) hydrogen peroxide, methanol, ethanol (100%), dimethylsulfoxide (DMSO), and acetone were purchased from Aldrich. Bovine erythrocyte superoxide dismutase (SOD) and *tert*-butyl hydroperoxide were obtained from Sigma. DEPMPO (5-diethoxy-phosphoryl-5-methyl-1-pyrroline-*N*-oxide) was obtained from Oxis International (Portland, OR) and DIPPMPPO (5-diisopropoxy-phosphoryl-5-methyl-1-pyrroline-*N*-oxide) was synthesized as described below. Water used in sample preparation was distilled and deionized.

4.2. Synthesis of DIPPMPPO

DIPPMPPO was synthesized according to a modified two-step procedure, in which the catalytic amount of the Lewis acid, boron trifluoride diethyl etherate, was added to shorten the reaction time of diisopropyl-(2-methylpyrrolidin-2-yl) phosphonate from 12 days to 3 days in high yield (96%). It was then oxidized with H_2O_2 using catalytic amounts of Na_2WO_4 . After purification by silica column ($\text{CH}_2\text{Cl}_2/\text{EtOH} = 10:1$, v/v) or recrystallization, the desired product was isolated. Scheme 5 shows the synthetic steps.

Diisopropyl(2-methylpyrrolidin-2-yl)phosphonate. 2-Methylpyrroline was previously purified by distillation, with 5 Å molecular sieves at 40°C under 20 mm Hg. After purification, 2-methylpyrroline (16.0 mL, 151.6 mmol, 1.0 equiv.) was placed in a 100 mL septa sealed flask, which was previously oven dried and filled with nitrogen via syringe. Diisopropyl phosphite (28.4 mL, 166.8 mmol, 1.1 equiv.) was then added, as well as a catalytic amount of boron trifluoride diethyl etherate (1.76 mL, 14.1 mmol, 0.093 equiv.), both via syringe too. This mixture was then allowed to stir at room temperature for 72 h under nitrogen. The product was poured into a HCl solution (1 N, 120 mL) and mixed by gentle agitation. This solution was then washed with methylene chloride (200 mL) using a separating funnel. The organic phase containing the unreacted starting material was discarded and the aqueous phase was made alkaline using saturated sodium carbonate solution (120 mL). The basic solution was extracted with chloroform ($40 \text{ mL} \times 3$). The combined organic phase was then dried using sodium sulfate and concentrated under vacuum using a vacuum pump. Diisopropyl (2-methylpyrrolidin-2-yl) phosphonate was obtained as a light colored oil (96%) and used without further purification in the second step of the synthetic procedure.

5-Diisopropylphosphoryl-5-methyl-1-pyrroline-N-oxide (DIPPMPPO). An aqueous solution of $\text{Na}_2\text{WO}_4 \cdot 2\text{H}_2\text{O}$ (4.12 g, 12.48 mmol, in 1.6 L of water) was mixed with diisopropyl (2-methylpyrrolidin-2-yl) phosphonate (32 mL, 303.2 mmol) in a 3.0 L reactor at 0°C . A 30% solution of hydrogen peroxide (60 mL, 921 mmol) was added dropwise over 1.5 h with stirring at 0°C . The sample was then kept for an additional 48 h at a temperature of 0°C in the refrigerator. After this time, the mixture was extracted into chloroform ($100 \text{ mL} \times 5$) and set aside. The remaining aqueous layer was saturated with brine and subsequently extracted using an additional 500 mL of chloroform. The organic phases were then combined and dried over sodium sulfate for a period of 12 h at 0°C . The solvent was then removed under vacuum. The crude product, dissolved in chloroform ($\sim 0.3 \text{ g L}^{-1}$), was purified by Flash chromatography (Biotage-SP1, column: Biotage Si 25 + M 1462-2; flow rate: 25 mL min^{-1} ; UV detection: 254 nm; gradient: methylene chloride/ethanol (100 until 90:10)). The solvent from the collected fraction containing the pure product was evaporated under dark in a rotary evaporator using at room temperature. After all the synthesis and purification procedures, 50% by weight of an amber-colored solid was obtained. The quality of the product was then evaluated using ^{31}P and ^1H NMR spectroscopies. The ^{31}P NMR spectra showed a single resonance at 22.2 ppm, in agreement with the literature.⁸



Scheme 5. Synthesis of DIPPMPPO.

The chemical shifts as well as the multiplicities for the proton resonances were: 7.10 ppm singlet N=CH, 4.60 ppm multiplet CH, 2.6 ppm multiplet CH₂, 2.05 ppm multiplet CH₂, 1.45 duplet CH₂, and 1.20 ppm duplet CH₂, consistent with literature citations.⁸ The spin trap was stored under argon at -70 °C.

4.3. Generation of free radicals for NMR measurements

4.3.1. Hydroxyl radicals. *Photolysis of H₂O₂.* Photolysis of H₂O₂ was used to generate hydroxyl radicals. A solution of DIPPMPPO or DEPMPO (68 mmol L⁻¹) and H₂O₂ (2.5 mmol L⁻¹) in sodium hydrogen phosphate buffer (30 mmol L⁻¹, pH 7.4) containing DTPA (4 mmol L⁻¹) was prepared and the reaction mixture transferred to a quartz cuvette. The sample was then irradiated with a 450 W medium pressure mercury-vapor lamp (Ace Glass Incorporated, Serial No. 7825-34, 222.4–1367.3 nm), which was used as the UV light source. The formation of radical species was monitored as a function of irradiation time.

Fenton system. A solution of DIPPMPPO (30 mmol L⁻¹) and different concentrations of the Fenton system, in the range 2–8 mmol L⁻¹ of FeSO₄ (ratio of H₂O₂/Fe²⁺ was 1000/1), in a buffer containing DTPA (25 mmol L⁻¹) were reacted in the dark for 2 h.

4.3.2. Superoxide/hydroperoxyl radicals. *Reaction of H₂O₂ with O₂ under alkaline conditions.* Different concentrations of H₂O₂ were used to generate superoxide radicals in contact with oxygen under alkaline conditions. DIPPMPPO (100 mmol L⁻¹) was added to form the DIPPMPPO/OOH adducts. The reaction mixture was stirred continuously in air for 20 min in the dark. The formation of radical species was monitored as a function of variable amounts of H₂O₂.

Photolysis of H₂O₂. Photolysis of 30% H₂O₂ was also used to generate superoxide radicals. The procedure is the same as above. When UV irradiation was not required, solid KO₂ dissolved in water was used as a source of superoxide.

4.3.3. Methyl radicals. Photolysis of *tert*-butylhydroperoxide (70% in water) or dimethylsulfoxide (DMSO) in 3% hydrogen peroxide was used to generate methyl radicals. DIPPMPPO or DEPMPO (68 mmol L⁻¹) was added to either *tert*-butylhydroperoxide or 3% H₂O₂ containing DMSO and the reaction mixture transferred to a quartz cuvette. The sample was then irradiated with a 450 W medium pressure mercury-vapor lamp. The formation of radical species was monitored as a function of irradiation time.

4.3.4. Hydroxyalkyl radicals. Hydroxymethyl and hydroxyethyl radicals were generated by hydroxyl radical-induced hydrogen abstraction from methanol and ethanol, respectively. Hydroxyl radicals were produced by UV irradiation (450 W medium pressure mercury-vapor lamp) of the appropriate alcohol in 3% H₂O₂.

4.4. Trapping free radicals from H₂O₂ as a function of pH

DIPPMPPO (68 mmol L⁻¹) was introduced into aqueous solutions of peroxide in acidic, neutral or alkaline pH. Buffer solutions were used in all experiments: pH 4 (0.05 mol L⁻¹ potassium biphthalate), pH 6 (0.05 mol L⁻¹ potassium phosphate monobasic sodium hydroxide), pH 7 (0.03 mol L⁻¹ sodium hydrogen phosphate), pH 9 (0.05 mol L⁻¹ sodium bicarbonate, 0.1 mol L⁻¹ sodium hydroxide, and hydrochloric acid), and pH 10 and 11 (0.05 mol L⁻¹ sodium bicarbonate and 0.1 mol L⁻¹ sodium hydroxide). These reaction systems were purged of air with nitrogen and stirred at room temperature for 90 min. The samples were then examined using ³¹P NMR spectroscopy.

4.5. ³¹P NMR spectra

³¹P NMR spectra were acquired on a Bruker-300 and a Varian XL-200 MHz spectrometers (operating at 121, 49, and 80.99 MHz, respectively). The chemical shifts reported are relative to external *ortho*-phosphoric acid (85%). All spectra were acquired with proton decoupling. The total number of scans for all experiments was 256–1024 with an acquisition time of 1.60 s. Trimethylphosphate was used as the internal standard for quantification and was added to the sample prior to measurement. The relaxation time (*T*₁) of the internal standard was measured and was determined to be approximately 13.5 s. In order to decrease the relaxation time, a relaxation agent (chromium chloride) was added to the mixture. With the addition of chromium chloride (30–35 mmol L⁻¹) to the samples prior to NMR measurement, the relaxation time of the phosphorus nuclei was decreased to ~200 ms. 5*T*₁ was used for the pulse delay.

4.6. Gas chromatography/mass spectrometry (GC/MS)

Structural analyses were performed using a Hewlett Packard 5972 mass spectrometer interfaced to a Hewlett Packard 5890-A gas chromatograph equipped with a DB-5 30 m × 0.25 mm capillary column.

4.7. Mass spectrometry

Mass spectrometry (MS) analyses were carried out on a KRATOS analytical MS25RFA mass spectrometer at 70 eV. The source temperature was 200 °C or a Finnigan LC Q Duo (ESI) mass spectrometer. Samples were freeze-dried prior to MS analyses.

The major mass spectrometric fragmentation patterns, after GC/MS analysis, for the superoxide radical adduct with DIPPMPPO were as follows: *m/z* (relative intensity %): 296(M-1, 10%), 254(100%), 212(8%). The major mass spectrometric fragmentation pattern, after MS/MS analysis, for the same superoxide radical adduct was as follows: *m/z* (relative intensity %): 297(M-1, 10%), 267(8%), 251(6%), 166(22%), 139(41%), 125(67%), 99(81%), and 60(65%).

The MS spectrum for the spin trapping of $\cdot\text{CH}_3$ with DIPPMPPO showed the following major fragmentation pattern: m/z (relative intensity %): 277(M–1, 80%), 235(4%), 193(31%), 176(12%), 112(100%), 96(35%), and 55(23%).

References and notes

1. Finkelstein, E.; Rosen, G. M.; Rauckman, E. *Mol. Pharmacol.* **1979**, *16*, 676.
2. Janzen, E. G. *Can. J. Chem.* **1978**, *56*, 2237.
3. Buettner, G. R.; Mason, R. P. *Methods Enzymol.* **1990**, *186*, 127.
4. Dikalov, S. I.; Mason, R. P. *Free Radicals Biol. Med.* **1999**, *27*, 864.
5. Khramstov, V.; Berliner, L. J.; Clanton, T. L. *Magn. Res. Med.* **1999**, *42*, 228.
6. Khramstov, V.; Berliner, L. J.; Clanton, T. L. *Supramol. Struct. Funct.* **2001**, *7*, 107.
7. Frejaville, C.; Karoui, H.; Le Moigne, F.; Culcasi, M.; Pietri, S.; Tordo, P. *French Patent No. PV 9308906*, 20 July, **1993**.
8. Chalier, F.; Tordo, P. *J. Chem. Soc., Perkin Trans. 2* **2002**, 2110.
9. Buettner, G. R. In *CRC Handbook of Methods for Oxygen Radical Research*; Greenwald, R. A., Ed.; CRC Press: Boca Raton, 1985; pp. 151–155.
10. Tsai, P.; Pou, S.; Rosen, G. M. *J. Chem. Soc., Perkin Trans. 2* **1999**, 1759.
11. Lloyd, R. V.; Hanna, P. M.; Mason, R. P. *Free Radicals Biol. Med.* **1997**, *5*, 885.
12. Rosen, G. M.; Turner, M. J., III *J. Med. Chem.* **1988**, *31*, 428.
13. Petlicki, J.; van de Ven, T. G. M. *J. Chem. Soc. Faraday Trans.* **1998**, *94*, 2763.
14. Sawyer, D. T.; Valentine, J. S. *Acct. Chem. Res.* **1981**, *14*, 393.
15. Karoui, H.; Nsanzumuhire, C.; Le Moigne, F.; Tordo, P. *J. Org. Chem.* **1999**, *64*, 1471.
16. Barbati, S.; Clement, J. L.; Olive, G.; Roubaud, V.; Tuccio, B.; Tordo, P. In *Free Radicals in Biology and Environment*; Minisci, F., Ed.; 1997; pp 39–47, 39.
17. Tordo, P. *Electron Paramagnetic Reson.* **1998**, *16*, 116.
18. Frejaville, C.; Karoui, H.; Tuccio, B.; Le Moigne, F.; Culcasi, M.; Pietri, S.; Lauricella, R.; Tordo, P. *Soc. Chem. Commun.* **1994**, *2*, 1793.
19. Frejaville, C.; Karoui, H.; Tuccio, B.; Le Moigne, F.; Culcasi, M.; Pietri, S.; Lauricella, R.; Tordo, P. *J. Med. Chem.* **1995**, *38*, 258.
20. Samuni, A.; Murali Krishna, C.; Riesz, P.; Finkelstein, E.; Russo, A. *Free Radicals Biol. Med.* **1989**, *6*, 141.
21. Roubaud, V.; Sankarapandi, S.; Kuppusamy, P.; Tordo, P.; Zweier, J. C. *Analytical Biochemistry* **1997**, *247*, 404.
22. Abbot, J.; Brown, D. G. *Can. J. Chem.* **1990**, *68*, 1537.
23. Janzen, E. G.; Zhang, Y.-K. *J. Org. Chem.* **1995**, *60*, 5441.
24. Kotake, Y.; Kuwata, K.; Janzen, E. G. *J. Phys. Chem.* **1979**, *83*, 3024.
25. Reinke, L. A.; Kotake, Y.; McCay, P. B.; Janzen, E. G. *Free Radicals Biol. Med.* **1991**, *11*, 31.
26. Pou, S.; Ramos, C. L.; Gladwell, T.; Renks, E.; Centra, M.; Young, D.; Cohen, M. S.; Rosen, G. M. *Anal. Biochem.* **1994**, *217*, 76.
27. March, J. *Advanced Organic Chemistry; Reaction, Mechanisms and Structure*, 3rd ed.; 1985; Chapter 7.
28. Bors, W.; Tait, D.; Michel, C.; Saran, M.; Erben-Russ, M. *Israel J. Chem.* **1984**, *24*, 17.